Title:

Proteomic analysis of the secretome of human bone marrow-derived Mesenchymal Stem Cells primed by pro-inflammatory cytokines

Authors:

Elisa Maffioli [a,b], Nonnis Simona [a,b], Roberta Angioni [c,d], Fabiana Santagata [a,b], Bianca Calì [c,d], Lucia Zanotti [e], Armando Negri [a,b], Antonella Viola [c,d*], Gabriella Tedeschi [a,b*]

Affiliations:

[a] Università degli Studi di Milano, Dipartimento di Medicina Veterinaria, via Celoria 10, 20133, Milano, Italy

[b] Fondazione Filarete, Viale Ortles 22/24, 20139 Milano, Italy

[c]Università di Padova, Dipartimento di Scienze Biomediche, Via Ugo Bassi, 58/b, 35131- Padova, Italy

[d] VIMM- Istituto Veneto di Medicina Molecolare, Via Orus, 2, 35129 – Padova, Italy

[e] Division of Regenerative Medicine, Stem Cells and Gene Therapy, San Raffaele Hospital, Milano, Italy.

* Corresponding authors:

Gabriella Tedeschi at Università degli Studi di Milano, Dipartimento di Medicina Veterinaria, via Celoria 10, 20133, Milano, Italy, mail: gabriella.tedeschi@unimi.it

Antonella Viola at Università di Padova, Dipartimento di Scienze Biomediche, Via Ugo Bassi, 58/b, 35131- Padova, Italy, mail: antonella.viola@unipd.it

Abstract

Mesenchymal stem cells (MSC) represent an impressive opportunity in term of regenerative medicine and immunosuppressive therapy. Although it is clear that upon transplantation MSC exert most of their therapeutic effects through the secretion of bioactive molecules, the effects of a pro-inflammatory recipient environment on MSC secretome have not been characterized. In this study, we used a label free mass spectrometry based quantitative proteomic approach to analyze how pro-inflammatory cytokines modulate the composition of the human MSC secretome. We found that pro-inflammatory cytokines have a strong impact on the secretome of human bone marrow-derived MSC and that the large majority of cytokine-induced proteins are involved in inflammation and/or

angiogenesis. Comparative analyses with results recently obtained on mouse MSC secretome stimulated under the same conditions reveals both analogies and differences in the effect of pro-inflammatory cytokines on MSC secretome in the two organisms. In particular, functional analyses confirmed that tissue inhibitor of metalloproteinase-1 (TIMP1) is a key effector molecule responsible for the anti-angiogenic properties of both human and mouse MSC within an inflammatory microenvironment. Mass spectrometry data are available via ProteomeXchange with identifier PXD005746

Significance

The secretion of a broad range of bioactive molecules is believed to be the main mechanism by which MSC exert specific therapeutic effects. MSC are very versatile and respond to specific environments by producing and releasing a variety of effector molecules. To the best of our knowledge this is the first study aimed at describing the secretome of human MSC primed using a mixture of cytokines, to mimic pro-inflammatory conditions encountered in vivo, by a quantitative high-resolution mass spectrometry based approach. The main output of the study concerns the identification of a list of specific proteins involved in inflammation and angiogenesis which are overrepresented in stimulated MSC secretome. The data complement a previous study on the secretome of mouse MSC stimulated under the same conditions. Comparative analyses reveal analogies and differences in the biological processes affected by overrepresented proteins in the two organisms. In particular, the key role of TIMP-1 for the anti-angiogenic properties of stimulated MSC secretome already observed in mouse is confirmed in human. Overall, these studies represent key steps necessary to characterize the different biology of MSC in the two organisms and design successful pre-clinical experiments as well as clinical trials.

Keywords: secretome; MSC; stem cells; mass spectrometry; TIMP-1

1. Introduction

Mesenchymal stem cells (MSC) are a heterogeneous population of adherent cells with a self-renewable capacity and with a wide distribution in an adult organism; indeed, they can be isolated from several adult tissues including bone marrow, adipose tissue, kidney and liver [1].

As multipotent progenitor cells, depending on the stimulus and the culture conditions employed, MSC are able to differentiate into various cell types, especially of the mesodermal lineage. The maintenance of stem cell subsets in adult tissues has been suggested as the physiological role of

MSC, especially in the context of bone marrow. The localization of MSC in vivo indicates that they are fundamental components of the perivascular niche, controlling maintenance and trafficking of Hematopoietic Stem Cells (HSC) and immune cells [2].

Besides their physiological role, MSC represent an impressive opportunity in term of regenerative medicine and immunosuppressive therapy. Indeed, in vitro studies demonstrated the ability of MSC to inhibit proliferation and activation of a large number of immune cells such as T cells, B-cells, natural killer cells (NK) and dendritic cells (DC) [3]. The secretion of a broad range of bioactive molecules is now believed to be the main mechanism by which MSC exert specific effects [4]. Thus, it has become increasingly important to achieve a complete qualitative and quantitative characterization of MSC secretome by –omics approaches, as confirmed by the large number of recent studies aimed at characterizing the secretome of MSC primed under different conditions [5-18]. Indeed, several studies have demonstrated that MSC are very versatile and respond to the environment by producing and releasing a variety of effector molecules [19]. This is a crucial issue when considering MSC-based therapy, because the biological activity of the transplanted cells will be strongly influenced by the inflammatory status of the host [20]. In this regard, we have recently published a paper reporting the employment of a high-throughput proteomic approach to detect the specific proteins whose expression is modulated when mouse MSC (mMSC) are primed by pro-inflammatory cytokines [21]. The main result of our study was the observation that pro-inflammatory stimulation results in up-regulation in the mMSC secretome of a number of both pro- and anti-angiogenic proteins. Amongst the latter, TIMP-1 - an endogenous inhibitor of metalloproteinases - was pinpointed as a key factor for the anti-angiogenic and anti-inflammatory effects exerted by the stimulated mMSC [21].

Human MSC (hMSC) are currently being tested in a wide range of clinical settings, mainly in autoimmune diseases (multiple sclerosis, rheumatoid arthritis, Crohn's disease, etc.), graft-versus-host disease (GvHD), wound repair, ischaemia/stroke, liver diseases and HSC engraftment. Despite the large number of ongoing clinical trials, the demonstration of a beneficial effect from hMSC in large placebo-controlled trials remains elusive. In some cases, hMSC have even been reported to lead to the exacerbation of disease symptoms [22, 23]. Among the reasons responsible for this inconsistency, there might be differences in the responses of mouse and human MSC to the inflammatory milieu. Indeed, pre-clinical experiments in mice that are based on the use of either human or mouse MSC have important limitations: when human cells are transplanted in the mouse, it is possible that some of the cross-talks between MSC and the host are impaired and that this may strongly affect the therapeutic effects of MSC transplantation; on the other hand, mMSC may have different biological properties than hMSC. Understanding the biology of human and mouse MSC is

therefore necessary to design and perform successful pre-clinical experiments as well as clinical trials.

To the best of our knowledge, the present study reports for the first time a quantitative proteomic characterization of the secretome of human, bone marrow-derived MSC primed with pro-inflammatory cytokines. Proteomic analyses were conducted under exactly the same conditions used in our previous investigation on mMSC in order to avoid variations with methodology, allowing direct comparative analysis between the results obtained with the two organisms.

2. Material and methods

2.1 Isolation of mMSC

mMSC were isolated as described [21] by flushing the femurs and tibias from 8 week-old, C57Bl/6N female mice and cultured in 25 cm^2 tissue culture flasks at a concentration of $2X10^6$ cells/cm^2 using complete Dulbecco modified Eagle medium low glucose (DMEM, Lonza, Braine-L'Alleud, Belgium) supplemented with 20% heat inactivated fetal bovine serum (Biosera, Ringmer, United Kingdom), 2 mM glutamine (Lonza), 100 U/mL penicillin/streptomycin (Lonza). Cells were incubated at 37°C in 5% CO_2. After 48 hours, the non-adherent cells were removed. After reaching 70–80% confluence, the adherent cells were trypsinized (0.05% trypsin at 37°C for 3 minutes), harvested and expanded in larger flasks. MSC at passage 10 were screened by flow cytometry for the expression of CD106, CD45, CD117, CD73, CD105, MHC-I, SCA-1 and CD11b and used to perform experiments (BD Pharmingen, Oxford, UK).

2.2 Collection of conditioned medium (CM) of mMSC

mMSC were plated as described [21] and let grow until confluence in ventilated cap flask. Growth medium was substituted with DMEM low glucose supplemented with 10% FBS, 2 mM glutamine, 100 U/mL penicillin/streptomycin, with (st mMSC) or without (unst mMSC) 25 ng/mL mIL1b, 20 ng/mL mIL6, 25 ng/mL mTNFa for 24 hours. After three washes in DMEM low glucose, the medium was changed with DMEM low glucose supplemented with 2 mM glutamine, 100 U/mL penicillin/streptomycin for the following 18 hours. Conditioned medium was harvested and centrifuged at 4000 rpm for 10 min.

2.3 Isolation of hMSC

hMSC were provided by Orbsen Therapeutics Ltd (Galway, Ireland). Ethical approvals are granted from the NUIG Research Ethics Committee and the Galway University Hospitals Clinical Research

Ethics Committee (CREC). Briefly, bone marrow was harvested from volunteers, and the cell culture was set up as previously described [24]. hMSC were characterized according to international guidelines [25]. All samples were obtained with informed consent. Procurement of the sample conformed to European Parliament and Council directives (2001/20/EC; 2004/23/EC).

2.4 Collection of conditioned medium (CM) of hMSC

hMSC were plated in with MEM Alpha with Glutamax supplemented with 10% FBS, 2 mM glutamine, 100 U/mL penicillin/streptomycin and let grow until confluence in in a humidified incubator with 5% CO_2 and 37°C. At the moment of the confluence, medium was substituted with MEM Alpha with Glutamax supplemented with 2% FBS, 2 mM glutamine, 100 U/mL penicillin/streptomycin, with (st hMSC) or without (unst hMSC) 25 ng/mL hIL1b, 20 ng/mL hIL6, 25 ng/mL hTNFa. 24 hours later, after three washes in MEM Alpha with Glutamax, the medium was changed with MEM Alpha with Glutamax supplemented with 2 mM glutamine, 100 U/mL penicillin/streptomycin for the following 18 hours. Conditioned medium was harvested and centrifuged at 4000 rpm for 10 min.

2.5 Endothelial Cell lines

SVEC4-10 (ATCC #CRL-2181 Manassas, VA), an endothelial cell line from murine axillary lymph nodes, was cultured in a humidified incubator with 5% CO_2 and 37°C, in DMEM (ATCC 30-2002 Manassas, VA) supplemented with 10% heat-inactivated FBS, 1% penicillin and streptomycin. Human Umbilical Vein Endothelial Cells (HUVEC, Lonza C2519A) were cultured in a humidified incubator with 5% CO_2 and 37°C with EBM-2 Basal Medium supplemented by EGM-2 BulletKit (CC-3156 & CC-4176). All the plastics used for HUVEC culture were pre-coated with 0.2% gelatin in H_2O (37°C for at least 2 hours). Cells were subcultured using 0.05% trypsin, 0.02% EDTA solution.

2.6 Tube formation assay SVEC4-10

Matrigel Matrix (Corning) was thawed overnight at 4°C. Tips and 96-well plates flat bottom were pre-chilled overnight before performing the experiment. The day of the assay, 80 µl of Matrigel were seeded in the 96-well plate and left to polymerize at 37°C, 5% CO_2 for at least 30 minutes. $1{,}5 \times 10^4$ SVEC4-10 were first suspended in 100µl of MSC-CM, supplemented with 10% FBS, alone or with anti-TIMP-1 (AF980 R&D) at the final concentration of 5 ug/mL, and then seeded on the solidified matrix. The formation of the tube networks develops in 4 hours at 37°C 10% CO_2. DMEM low glucose supplemented with 10% heat-inactivated FBS were used as positive control. At

the end of the incubation, cell tubes were imaged with a phase contrast inverted microscope at 4× objective magnifications and analysis was performed with ImageJ Angiogenesis Analyzer.

2.7 Tube formation assay HUVEC

Matrigel Matrix (Corning) was thawed overnight at 4°C. The day of the assay, 100 µl of Matrigel were seeded in the 96-well plate and left to polymerize at 37°C, 5% CO_2 for at least 30 minutes. $2x10^4$ HUVEC were first suspended in 100 µl of hMSC-CM, supplemented with 10% FBS, alone or with anti-TIMP-1 (AF970 R&D) at the final concentration of 5 ug/mL, and then seeded on the solidified matrix. The formation of the tube networks develops in 4 hours at 37°C 10% CO_2. MEMalpha supplemented with 10% heat-inactivated FBS were used as positive control. At the end of the incubation, cell tubes were imaged with a phase contrast inverted microscope at 4× objective magnifications and analysis was performed with ImageJ Angiogenesis Analyzer.

2.8 Isolation and Differentiation of Mouse Bone Marrow–Derived Monocytes

Bone marrow cell suspensions were obtained by flushing femurs and tibias of 8- to 12-week-old C57Bl/6N mice (Charles River; Sulzfeld, Germany) with complete DMEM low Glucose supplemented with 10% FCS, 1% Pen/Strep and 1% L-Glutamine. Possible cellular aggregates were removed by pipetting and red cells were eliminated through ACK lysis buffer (10-548E, Lonza). Cells were washed twice with medium, seeded on 24-well plates (Corning Costar; Schiphol-Rijk, the Netherlands) at the concentration of 10^6cells/mL and maintained in a humidified incubator with 5% CO_2 and 37°C.

Cells were supplemented with 20 ng/mL mM-CSF as positive control, or cultured in mMSC-CM supplemented with 10% FBS. MSC-CM and mM-CSF were replaced three days later. Cells were harvested five days later by gentle pipetting and repeated washing with phosphate buffered saline (PBS), and 2 mM EDTA. Monocytes differentiation was analysed by flow cytometry.

2.9 Isolation and differentiation Human Blood-Derived Monocyte

Peripheral Blood Monocyte Cells (PBMCs) from healthy donors were isolated by centrifugation on Ficoll-Paque solution and placed on Percoll 46% vol/vol solution (Amersham Biosciences) in RPMI 1640–10% FCS and 4 mM. Monocytes were harvested, resuspended in medium–2% FCS, and let to adhere to plastic (1 hour at 37°C) in order to eliminate contaminating lymphocytes. For macrophage differentiation, 3×10^5 monocytes were seeded in 24-well plates with MEMalpha supplemented with 20% FBS in the presence of 100 ng/mL h-M-CSF as positive control, or they

were cultured in hMSC-CM plus 20% FBS. After five days of differentiation, monocyte-derived macrophages were analysed by flow cytometry using CD14 staining.

2.10 Flow Cytometry analysis

The expression of macrophage surface markers was evaluated by Flow Cytometry analysis. Briefly, cells were washed and stained in PBS supplemented with 2% fetal calf serum. After 20 minutes of incubation at 4°C with Purified Rat Anti-Mouse CD16/CD32 (Mouse BD Fc BlockTM 553142), fluorescent antibodies were diluted in PBS supplemented with 2% fetal calf serum, to identify mouse macrophages (CD11b:PeCy7 BD 552850 and F4/80:Alexa Fluor® 488 BioRad MCA497F) and human macrophages (CD14: PE R&D FAB3832P). Cell viability was assessed with the Live/Dead Fixable Aqua Dead Cell Stain Kit (Invitrogen), following the manufacturer's instructions. After the final wash, cells were fixed in 1% paraformaldehyde and acquired with the BD FACSCanto™ II system. Post-analysis of flow cytometry data was performed using FlowJo™ software (Tree Star Inc.).

2.11 ELISA-Assay

To detect M-CSF and TIMP-1 concentration in MSC-CM, ELISA assays were performed following the manufacturer's instruction (for human, M-CSF DuoSet ELISA DY216 and TIMP-1 DuoSet ELISA DY970; for mouse, M-CSF DuoSet ELISA DY416 and TIMP-1 DuoSet ELISA DY980).

2.12 LC-ESI MS/MS analysis

Five technical replicas, including steps for sample preparation and mass spectrometric analysis, were performed for each sample (st hMSC-CM from patient H30, unst hMSC-CM from patient H30, st hMSC-CM from patient H34, unst hMSC-CM from patient H34).

Proteomic analyses were performed as described [21]. Briefly, proteins were precipitated with 10 % tricholoracetic acid for 2 h on ice, reduced, carbamydomethylated and digested with trypsin sequence grade trypsin (Roche) for 16 h at 37 °C using a protein:tripsin ratio of 50:1. Nano LC-ESI-MS/MS analysis was performed on a Dionex UltiMate 3000 HPLC System with a PicoFrit ProteoPrep C18 column (200 mm, internal diameter of 75 µm) (New Objective, USA) Gradient:1% ACN in 0.1 % formic acid for 10 min, 1-4 % ACN in 0.1% formic acid for 6 min, 4-30% ACN in 0.1% formic acid for 147 min and 30-50 % ACN in 0.1% formic for 3 min at a flow rate of 0.3 µl/min. The eluate was electrosprayed into an LTQ Orbitrap Velos (Thermo Fisher Scientific, Bremen, Germany) through a Proxeon nanoelectrospray ion source (Thermo Fisher Scientific). The LTQ-Orbitrap was operated in positive mode in data-dependent acquisition mode to automatically

alternate between a full scan (m/z 350-2000) in the Orbitrap (at resolution 60000, AGC target 1000000) and subsequent CID MS/MS in the linear ion trap of the 20 most intense peaks from full scan (normalized collision energy of 35%, 10 ms activation). Isolation window: 3 Da, unassigned charge states: rejected, charge state 1: rejected, charge states 2+, 3+, 4+: not rejected; dynamic exclusion enabled (60 s, exclusion list size: 200). Data acquisition was controlled by Xcalibur 2.0 and Tune 2.4 software (Thermo Fisher Scientific).

Mass spectra were analyzed using MaxQuant software (version 1.3.0.5) [26]. The initial maximum allowed mass deviation was set to 6 ppm for monoisotopic precursor ions and 0.5 Da for MS/MS peaks. Enzyme specificity was set to trypsin, defined as C-terminal to arginine and lysine excluding proline, and a maximum of two missed cleavages were allowed. Carbamidomethylcysteine was set as a fixed modification, N-terminal acetylation and methionine oxidation as variable modifications. The spectra were searched by the Andromeda search engine against the human UniProt sequence database (release 2014_01). Protein identification required at least one unique or razor peptide per protein group. Quantification in MaxQuant was performed using the built in XIC-based label free quantification (LFQ) algorithm [27] using fast LFQ. The required false positive rate was set to 1% at the peptide and 1% at the protein level, and the minimum required peptide length was set to 6 amino acids.

2.14 Statistical and bioinformatics analyses

Statistical analyses were performed using the Perseus software (version 1.4.0.6 [28]). Only proteins present and quantified in at least 3 out of 5 technical repeats were considered as positively identified in a sample(st hMSC-CM from patient H30, unst hMSC-CM from patient H30, st hMSC-CM from patient H34, unst hMSC-CM from patient H34). T-test analysis of stimulated versus unstimulated technical replicas were conducted separately for samples from the two patients. Comparing the results obtained in the two analyses, proteins were considered differentially expressed in stimulated samples if they were present only in st- or in unst- hMSC-CM or showed significant t-test p-value (cut-off at 1% permutation-based False Discovery Rate) in both patients.

Proteins listed in Tables 1 and 2 and Supplemantal Table 2 were considered secreted or involved in inflammation/angiogenesis according to the following databases/datasets: Gene Ontology [29], NextProt [30], UniProt [31], Gene Cards [32], datasets [6, 8] and manual literature mining. Bioinformatic analyses were carried out by DAVID software (release 6.7) [33]. GOBP and groups were filtered for significant terms (modified Fisher exact EASE score p value <0.05 and at least five counts). Networks of up-regulated proteins in st hMSC-CM involved in inflammation or

angiogenesis was performed using String [34] **(**active interactions: text mining, experiments, databases).

The mass spectrometry proteomics data have been deposited to the ProteomeXchange Consortium via the PRIDE [35] partner repository with the dataset identifier PXD005746.

3. Results and Discussion

3.1 Proteomic characterization of hMSC secretome

Fig. 1 summarizes the results of the proteomic characterization of secretome of hMSC before and after stimulation with inflammatory cytokines; 497 proteins were present in at least 3 out of 5 technical replicas in at least one stimulation condition (stimulated or unstimulated) in both patients (donors H30 and H34). These proteins are listed in Supplemental Table 1, together with their main identification parameters. Fig.1A highlights the number of proteins detected in stimulated human MSC conditioned medium (st hMSC-CM) and unstimulated human MSC conditioned medium (unst hMSC-CM). Amongst the 465 proteins identified in st hMSC-CM (proteins in groups 1, 2, 4 and 5 of Supplemental Table 1), 133 are listed as cytokine or chemokine or functionally related to these classes of compounds according to the NextProt database [30].

3.2 Proteins up-regulated in stimulated hMSC-CM

Since MSC enhance their therapeutic efficacy following priming by cytokines [36, 37], analyses were focused on proteins overrepresented or present only in st hMSC compared to unst hMSC secretome; 39 proteins are present only in st hMSC-CM, while 426 are common to stimulated and unstimulated hMSC-CM (Fig. 1A); statistical analysis of the common proteins indicates that 57 proteins are overrepresented in st hMSC-CM (according to t-test -p-value, cut-off at 1% permutation-based False Discovery Rate). Overall, 96 proteins are up-regulated or present only in st hMSC-CM in both patients (Table 1, which reports the t-test p-values and t-test difference for each protein in each patient). Fig. 1B, showing the t-test differences calculated for each patient for the 57 up-regulated proteins present in both st- and unst-hMSC-CM , allows detecting proteins highest increase in abundance in in stimulated *versus* unstimulated hMSC-CM in each patient. A Pearson correlation coefficient R=0.73 was calculated from data in Fig. 1B.

All proteins listed in Table 1 are predicted to be potentially secreted/extracellular/included in exosomes according to annotations in Gene Ontology [29] or NextProt [30] or UniProt [31] or Gene Cards [32]) or in datasets [6, 8] or from manual literature mining.

70% and 64% of up-regulated proteins in st hMSC-CM are involved in inflammation or angiogenesis, respectively (Table 1). The extended network of interactions amongst inflammation- or angiogenesis-related proteins up-regulated in st hMSC-CM according to available experimental evidence, database and literature information is shown in Fig. 2. A number of proteases (BMP1, C1R, C1S, CFB, CTSB, MMP1, MMP2, MMP3, MMP10 MMP13, PSMA5, PSME2, QPCT) and protease inhibitors (C3, COL7A1, FBLN1, FN1INHBA, ITIH2, SERPINB2, SERPINE1, TIMP1) are up-regulated in st hMSC secretome, strengthening our suggestion that a fine but complex tuning of proteolytic activity is a key mechanism regulating MSC effects on angiogenesis and tissue remodeling [21]. In particular, MMPs are presently considered not only effectors but also regulators of a number of biological processes since they can activate, inactivate or antagonize the biological functions of growth factors, cytokines and chemokines by proteolytic processing and thus either promote or suppress inflammation and angiogenesis [38. 39]. Notably several protease/protease inhibitors listed above are amongst the proteins showing large quantitative differences in stimulated vs unstimulated hMSC-CM (Table 1, Fig. 1B and Fig. 2).

Since it has been established that tissue origin, growth and stimulation conditions may influence the type and quantity of proteic components of MSC secretome [16], we compared the list of up-regulated proteins in st hMSC-CM with those reported in recent studies performed using a similar mass spectrometry based quantitative proteomic approach on human MSC. Supplemental Table 2 confirms that different stimulation conditions lead to up-regulation of largely different sets of proteins. Notably, 24 proteins (25%, highlighted in Supplemental Table 2) detected as up-regulated in our study were overrepresented also in the secretome of MSC deriving from a different adult tissue (adipose tissue) stimulated with TNF-α [11]. This finding provides new experimental evidences at the molecular level supporting the notion that the type of stimulus has a major influence on MSC secretome. As expected, considering the stimulating agent, 22 out of 24 common overrepresented proteins are related to inflammation and/or angiogenesis (Supplemental Table 2).

3.3 Proteomic based comparison between mouse and human MSC-CM

In our previous work, we took advantage of animal models to elucidate the molecular pathway involved in effects of mMSC on the complex crosstalk between inflammation and angiogenesis [21]. Because it is widely accepted that significant differences exist between mouse and human MSC [36, 40], and because of the tremendous relevance of inflammation-induced angiogenesis in human diseases, we focused our attention on comparing mouse and human MSC secretome. The proteomic results of the present study were therefore compared with those reported for mMSC-CM [21]. Supplemental Table 1 lists the 286 proteins (out of 465, 62%) present in st hMSC-CM that

have been detected also in st mMSC-CM. The number of proteins significantly up-regulated or present only in the secretome of stimulated MSC is similar in the two species: 89 in mouse (Table S2 of [21]), 96 in human (Table 1). A comparative analysis of GO_BP category enrichment of overrepresented proteins in human and/or mouse (Fig. 3) suggests that: a) proteins up-regulated in the secretome of stimulated MSC from both organisms are, for the most part, involved in similar biological processes, mainly related to defense, immune and inflammatory response, chemotaxis and extracellular matrix remodeling; b) however there are clear important differences among human and mouse. Thus, only st mMSC-CM is enriched in proteins involved in chromatin structure assembly, cell proliferation regulation and related processes. On the contrary, complement activation, leukocyte migration, bone development and metabolic processes specifically related to collagen are amongst the statistically enriched GO functional categories in human but not in mouse. Such differences are confirmed by the observation that only 23 proteins are up-regulated or present only in stimulated MSC-CM both in mouse and human (Table 2); this again points to a fine species-related tuning of the overall effects of secretome from the two organisms; interestingly, our analysis indicates that 74 % and 83% of the common up-regulated proteins are associated with angiogenesis or inflammation, respectively.

3.4 Functional evidence of human and mouse MSC secretome similarities or differences

Our proteomic results indicate that the majority of secreted proteins from both human and mouse MSC are associated with inflammation and angiogenesis (Table 1 and [21]). To identify specific functional analogies or differences of human and mouse MSC in the regulation of these two important processes, we focused on two proteins, M-SCF/CSF1 and TIMP1, which are present in st MSC-CM of both species and play a key role in immunity/inflammation and angiogenesis, respectively [41, 42].

3.4.1 Macrophage colony-stimulating factor (M-CSF)

M-CSF is a growth factor secreted by a large variety of cells including macrophages, endothelial cells, fibroblast and lymphocytes. By interacting with its membrane receptor (CSF1R or M-CSF-R), it stimulates the survival, proliferation, and differentiation of monocytes and macrophages [43-45]. Our proteomic data indicated that M-CSF (CSF1) is up-regulated in the secretome of both human and mouse MSC upon stimulation by inflammatory cytokines (Tables 1 and 2 and Fig. 2). Thus, we investigated the ability of MSC-CM to generate monocyte-derived macrophages in vitro. Surprisingly, our data revealed an important difference between mouse and human MSC-CM (Fig. 4). When compared to the positive control (recombinant mouse M-CSF), both unst mMSC-CM or

st mMSC-CM were unable to induce macrophage differentiation (F4/80$^+$, CD11b$^+$ cells) efficiently. In this case, stimulation of mMSC with pro-inflammatory cytokines did not change the properties of the secretome (Fig. 4 A). In contrast, the culture of human monocytes in the presence of st hMSC-CM produced the same percentage of differentiated macrophages as the positive control (recombinant human M-CSF) (Fig. 4 B). These data reflect the amount of mouse or human M-CSF detectable by ELISA in unst or st human and mouse MSC-CM (Fig. 4). Thus, although M-CSF is up-regulated in both human and mouse MSC-CM upon stimulation by inflammatory cytokines, the amount of M-CSF secreted by mMSC is too low to be detected by ELISA and to induce macrophage differentiation efficiently.

Notably, proteomic data on human M-CSF (CSF1) fully agree with functional assays and ELISA analysis. As reported in Table 1 and Fig. 2, M-CSF is amongst the proteins showing the highest increase/present only in stimulated human secretome according to mass spectrometric analysis; the apparent discrepancy in the presence of CSF1 in unst hMSC-CM between ELISA (showing low levels of M-CSFin unst hMSC-CM, Fig. 4) and proteomics (listing M-CSF as absent in unst hMSC-CM in Table 1) is due to the high stringency used to filter quantitative proteomic data in the present report (detection in at least 3 out of 5 technical replicas in both patients). In fact, M-CSF was detected also in low amounts in 4 out of 5 replicas of unstimulated secretome of donor H34 but only in 2 out of 5 replicas of donor H30 and consequently listed as “non detected” in unst hMSC-CM.

3.4.2 TIMP-1

Concerning angiogenesis, in our previous work [21] we analysed the effect of mMSC-CM on *in vitro* angiogenesis exploiting the tube formation assay. As we reported in Fig. 5 A, soluble factors released by stimulated mMSC strongly inhibited the ability of SVEC4-10 cells, a mouse endothelial cell line, to form tube networks. In contrast, unst mMSC-CM had no effect on tube formation. In an effort to assess the angiogenetic role of hMSC, we performed the same experiments using HUVEC cells (Human Umbilical Vein Endothelial Cells) (Fig. 5 B). In agreement with the data obtained with mMSC, soluble factors secreted by hMSC affected the ability of HUVEC cells to form tubes. Interestingly, in the case of human cells, MSC-CM was able to inhibit tube formation even when MSC had not been primed by cytokines. However, pre-activation with pro-inflammatory cytokines strengthened the anti-angiogenic effects of hMSC-CM, thus supporting our hypothesis that, during an inflammatory response, MSC target angiogenesis and thus dampen the inflammatory response [21].

Using both in vitro and in vivo approaches, we demonstrated that mMSC anti-angiogenic effect is mediated by TIMP-1 [21]. Because the proteomic analyses indicate that TIMP-1 is one of the

proteins up-regulated in both human and mouse st MSC-CM (Table 2), we compared the results obtained by blocking TIMP-1 in SVEC4-10 cells incubated in the presence of mMSC-CM (Fig. 6 A) with those generated using HUVEC cells and hMSC-CM (Fig. 6 B). By inhibiting TIMP-1 activity with a specific blocking antibody, we observed the complete recovery of HUVEC cell ability to form tubes even in the presence of st hMSC-CM, indicating that TIMP1 is one of the key secreted molecules targeting endothelial cells in both mouse and human MSC.

TIMP-1 concentration was measured by ELISA in st and unst, human and mouse MSC-CM (Fig. 7 A for mouse and B for human). In accordance with our data of tubulogenesis showing that unst mMSC-CM has no effect on angiogenesis (Figs. 5 and 6, panel A), the concentration of TIMP-1 in mMSC-CM was about 5-times higher when cells had been primed by pro-inflammatory cytokines. Thus, in mouse MSC, the anti-angiogenic phenotype is acquired only after licensing with pro-inflammatory cytokines, i.e. when TIMP-1 levels rise from about 3 ng/mL to 25 ng/mL. In hMSC, however, the basal high level of secreted TIMP1 may explain the partial anti-angiogenic effect of the unst hMSC-CM (Figs. 5 and 6, panel B). In fact, in support of this hypothesis, TIMP-1 blockade restored the formation of the endothelial network in the presence of unst or st hMSC-CM.

Again, proteomic data fully agree with functional assays and ELISA results for human TIMP1. As reported in Fig. 2 and Table 1, this protein is listed amongst those overrepresented in st hMSC but showing relative lower level increase following stimulation. Additional bioinformatics analyses of proteomic data further support the observation that even relatively small changes in the level of TIMP1 can result in very significant modulation of secretome properties. First of all, its level will greatly influence the proteolytic potential of the secretome and, consequently, the overall activity of a number of secretome components, including proteins which level is not increased following stimulation and proteins not directly involved in inflammation and angiogenesis; secondly, but not less importantly, TIMP1 is functionally related to a number of overrepresented proteins in stimulated secretome besides proteases (Fig. 2 and Supplemental Table 3**)**, like cytokines and structural proteins (such as IL6, IL8, CCL2 CXCL12, COL3A1). The complete list of the 54 proteins of stimulated hMSC-CM functionally correlated to TIMP1 according to String [34] is reported in Supplemental Table 3.

4. **Conclusions**

The proteomic analysis of hMSC-CM and mMSC-CM confirms that exposure to pro-inflammatory cytokines results in significantly higher secretion of a number of immunomodulatory and angiogenesis-related proteins by MSC from both species. Notably, 62% of the proteins identified in st hMSC-CM were also identified in st mMSC-CM, clearly highlighting the existence of a common

signature in the secretome of human and mouse MSC. However, although human and mouse MSC show a similar proteomic signature in response to stimulation by pro-inflammatory cytokines, our data indicate that they may induce different biological responses. Thus, even if M-CSF is up-regulated in both human and mouse MSC-CM, only hMSC-CM induce macrophage differentiation efficiently because of its high concentration of M-CSF.

In both species, several up-regulated proteins are associated with angiogenesis. The extended network of interactions amongst inflammation and angiogenesis-related proteins in stimulated hMSC-CM makes it extremely difficult to assess the in vivo physiological importance of each factor. In particular, the presence of a number of protease and protease inhibitors implies the possibility of additional self-modulation of the properties of the various components of the secretome [39].

Although our data fully confirm the anti-angiogenic role of stimulated MSC for both mouse and human cells, at basal conditions MSC behavior is striking different. Indeed, while unst MSC-CM collected from mouse cells has no effect on tube formation, hMSC-CM significantly reduces angiogenesis in vitro. Finally, the anti-angiogenic role of TIMP-1 already observed in the mouse model was confirmed also using hMSC-CM: by inhibiting TIMP-1 activity with a specific blocking antibody, we observed the complete recovery of HUVEC cell ability to form tubes even in the presence of st hMSC-CM, indicating that TIMP1 is one of the key secreted molecules targeting endothelial cells in both mouse and human MSC.

Acknowledgments

This work was supported in part by grants from “Università degli Studi di Milano” Italy. The authors wish to thank also the European Union’s Seventh Framework Programme for research, technological development, and demonstration under grant agreement no. 602363 and the ERC Advanced Grant under grant agreement no. 322823.

We thank Dr. Francesca Grassi Scalvini for table preparation and Dr Steve Elliman from Orbsen Therapeutics Ltd, National University of Ireland, Galway, Ireland for providing human MSC.

Conflict of interest

All the Authors have declared no conflict of interest

References

[1] Nombela-Arrieta C, Ritz J, Silberstein LE. The elusive nature and function of mesenchymal stem cells. Nat Rev Mol Cell Biol 2011;12:126-31.

[2] Shi C, Jia T, Mendez-Ferrer S, Hohl TM, Serbina NV, Lipuma L, Leiner I, Li MO, Frenette PS, Pamer EG. Bone marrow mesenchymal stem and progenitor cells induce monocyte emigration in response to circulating toll-like receptor ligands. Immunity 2011;34:590-601.

[3] De Miguel MP, Fuentes-Julián S, Blázquez-Martínez A, Pascual CY, Aller MA, Arias J, Arnalich-Montiel. Immunosuppressive properties of mesenchymal stem cells: advances and applications. Curr Mol Med 2012;12:574-91.

[4] Kyurkchiev D, Bochev I, Ivanova-Todorova E, Mourdjeva M, Oreshkova T, Belemezova K, Kyurkchiev S. Secretion of immunoregulatory cytokines by mesenchymal stem cells. World J Stem Cells 2014;6:552-70.

[5] Kalinina N, Kharlampieva D, Loguinova M, Butenko I, Pobeguts O, Efimenko A, Ageeva L, Sharonov G, Ischenko D, Alekseev D, Grigorieva O, Sysoeva V, Rubina K, Lazarev V, Govorun V. Characterization of secretomes provides evidence for adipose-derived mesenchymal stromal cells subtypes. Stem Cell Res Ther 2015;6:221.

[6] Rocha B. Secretome analysis of human mesenchymal stem cells undergoing chondrogenic differentiation. J Proteome Res 2014;13:1045-54.

[7] Salgado AJ, Sousa JC, Costa BM, Pires AO, Mateus-Pinheiro A, Teixeira FG, Pinto L, Sousa N. Mesenchymal stem cells secretome as a modulator of the neurogenic niche: basic insights and therapeutic opportunities. Front Cell Neurosci 2015;9:249.

[8] Kristensen SP, Chen L, Overbeck Nielsen M, Qanie DW, Kratchmarova I, Kassem M, Andersen JS. Temporal Profiling and Pulsed SILAC Labeling Identify Novel Secreted Proteins During Ex Vivo Osteoblast Differentiation of Human Stromal Stem Cells. Mol Cell Proteomics 2012;989-1007.

[9] Kim JM, Kim J, Kim YH, Kim KT, Ryu SH, Lee TG, Suh PG. Comparative secretome analysis of human bone marrow-derived mesenchymal stem cells during osteogenesis. J Cell Physiol 2013;228:216-24.

[10] Choi YA, Lim J, Kim KM, Acharya B, Cho JY, Bae YC, Shin HI, Kim SY, Park EK. Secretome analysis of human BMSCs and identification of SMOC1 as an important ECM protein in osteoblast differentiation. J Proteome Res 2010;9:2946-56.

[11] Lee MJ, Kim J, Kim MY, Bae YS, Ryu SH, Lee TG, Kim JH. Proteomic analysis of tumor necrosis factor-alpha-induced secretome of human adipose tissue-derived mesenchymal stem cells. J Proteome Res 2010;9:1754-62.

[12] Kumar DJ, Holmberg C, Balabanova S, Borysova L, Burdyga T, Beynon R, Dockray GJ, Varro A. Mesenchymal Stem Cells Exhibit Regulated Exocytosis in Response to Chemerin and IGF. PLoS ONE 2015; 10:e0141331.

[13] De Boeck A, Hendrix A, Maynard D, Van Bockstal M, Daniëls A, Pauwels P, Gespach C, Bracke M, De Wever O. Differential secretome analysis of cancer-associated fibroblasts and bone marrow-derived precursors to identify microenvironmental regulators of colon cancer progression. Proteomics 2013;13:379-88.

[14] Yu S, Zhao Y, Ma Y, Ge L. Profiling the Secretome of Human Stem Cells from Dental Apical Papilla. Stem Cells Dev 2016;25:499-508.

[15] Amable PR, Teixeira MVT, Carias RBV, Granjeiro JM, Borojevic. Protein synthesis and secretion in human mesenchymal cells derived from bone marrow, adipose tissue and Wharton's jelly. Stem Cell Research & Therapy 2014;5:53.

[16] Clabaut A, Grare C, Léger T, Hardouin P, Broux O. Variations of secretome profiles according to conditioned medium preparation: The example of human mesenchymal stem cell-derived adipocytes. Electrophoresis 2015;36:2587-93.

[17] Bara JJ, Turner S, Roberts S, Griffiths G3, Benson R, Trivedi JM, Wright KT. High content and high throughput screening to assess the angiogenic and neurogenic actions of mesenchymal stem cells in vitro. Exp Cell Res 2015;333:93-104.

[18] Riis S, Stensballe A, Emmersen J, Pennisi CP, Birkelund S, Zachar V, Fink. Mass spectrometry analysis of adipose-derived stem cells reveals a significant effect of hypoxia on pathways regulating extracellular matrix. Stem Cell Res Ther 2016;7:52.

[19] Murphy MB, Moncivais K, Caplan AI. Mesenchymal stem cells: environmentally responsive therapeutics for regenerative medicine. Exp Mol Med 2013;45 e 54.

[20] Krampera M. Mesenchymal stromal cell 'licensing': a multistep process. Leukemia 2011;25:1408-14.

[21] Zanotti L, Angioni R, Calì B, Soldani C, Ploia C, Moalli F, Gargesha M, D'amico G, Elliman S, Tedeschi G, Maffioli E, Negri A, Zacchigna S, Sarukhan A, Stein JV, Viola A. Mouse mesenchymal stem cells inhibit high endothelial cell activation and lymphocyte homing to lymph nodes by releasing TIMP-1. Leukemia 2016;30:1143-54.

[22] Ankrum J, Karp JM. Mesenchymal stem cell therapy: Two steps forward, one step back. Trends in Molecular Medicine 2010;16:203-9.

[23] Kishk NA, Abokrysha NT, Gabr H. Possible induction of acute disseminated encephalomyelitis (ADEM)-like demyelinating illness by intrathecal mesenchymal stem cell injection. J Clin Neurosci 2013;20:310-2.

[24] McAuley DF, Curley GF, Hamid UI, Laffey JG, Abbott J, McKenna DH, Fang X, Matthay MA, Lee JW. Clinical grade allogeneic human mesenchymal stem cells restore alveolar fluid clearance in human lungs rejected for transplantation. Am J Physiol Lung Cell Mol Physiol 2014;306:L809-15.

[25] Dominici M, Le Blanc K, Mueller I, Slaper-Cortenbach I, Marini F, Krause D, Deans R, Keating A, Prockop Dj, Horwitz E. Minimal criteria for defining multipotent mesenchymal stromal cells. The International Society for Cellular Therapy position statement. Cytotherapy 2006;8:315-7.

[26] Cox J, Mann M. MaxQuant enables high peptide identification rates, individualized p.p.b.-range mass accuracies and proteome-wide protein quantification. Nat Biotechnol 2008;26:1367–72.

[27] Cox J, Hein MY, Luber CA, Paron I, Nagaraj N, Mann M. Accurate proteome-wide label-free quantification by delayed normalization and maximal peptide ratio extraction, termed MaxLFQ. Mol Cell Proteomics 2014;13:2513-26.

[28] Tyanova S, Temu T, Sinitcyn P, Carlson A, Hein MY, Geiger T, Mann M, Cox J. The Perseus computational platform for comprehensive analysis of (prote)omics data. Nat Methods 2016;13:731-40.

[29] The Gene Ontology Consortium. Gene Ontology Consortium: going forward. Nucl Acids Res 2015;43: D1049-56.

[30] Gaudet P, Michel PA, Zahn-Zabal M, Cusin I, Duek PD, Evalet O, Gateau A, Gleizes A, Pereira M, Teixeira D, Zhang Y, Lane L, Bairoch A. The neXtProt knowledgebase on human proteins: current status. Nucleic Acids Res 2015;43:D764-70

[31] The UniProt Consortium. UniProt: a hub for protein information. Nucleic Acids Res 2015;43:D204-12.

[32] Stelzer G, Rosen R, Plaschkes I, Zimmerman S, Twik M, Fishilevich S, Iny Stein T, Nudel R, Lieder I, Mazor Y, Kaplan S, Dahary, D, Warshawsky D, Guan-Golan Y, Kohn A, Rappaport N, Safran M, and Lancet D. The GeneCards Suite: From Gene Data Mining to Disease Genome Sequence Analysis. Curr Prot Bioinformatics 2016;54:1.30.1-1.30.33.

[33] Huang DW, Sherman BT, Lempicki RA. Bioinformatics enrichment tools: paths toward the comprehensive functional analysis of large gene lists. Nucleic Acids Res 2009;37:1-13.

[34] Szklarczyk D, Franceschini A, Wyder S, Forslund K, Heller D, Huerta-Cepas J, Simonovic M, Roth A, Santos A, Tsafou KP, Kuhn M, Bork P, Jensen LJ, von Mering C. STRING v10: protein-protein interaction networks, integrated over the tree of life. Nucleic Acids Res 2015;43: D447-52

[35] Vizcaíno JA, Csordas A, del-Toro N, Dianes JA, Griss J, Lavidas I, Mayer G, Perez-Riverol Y, Reisinger F, Ternent T, Xu QW, Wang R, Hermjakob H. 2016 update of the PRIDE database and related tools. Nucleic Acids Res 2016;44(D1): D447-56.

[36] Bernardo ME, Fibbe WE. Mesenchymal stromal cells: sensors and switchers of inflammation. Cell Stem Cell 2013;13:392-402.

[37] Groh ME, Maitra B, Szekely E, Koç ON. Human mesenchymal stem cells require monocyte-mediated activation to suppress alloreactive T cells. Exp Hematol. 2005;33:928-34.

[38] Nissinen L, Kahari VM. Matrix metalloproteinases in inflammation. Biochim Biophys Acta 2014;2571-80.

[39] Rodríguez D, Morrison CJ, Overall CM. Matrix metalloproteinases: What do they not do? New substrates and biological roles identified by murine models and proteomics. Biochim Biophys Acta 2010;1803:39-54.

[40] Romieu-Mourez R, Coutu DL, Galipeau J. The immune plasticity of mesenchymal stromal cells from mice and men: concordances and discrepancies. Front Biosci (Elite Ed) 2012; 4:824-37.

[41] John A. Hamilton. Colony-stimulating factors in inflammation and autoimmunity. Nature Reviews Immunology 2008;8(7):533-44.

[42] Qing Xiang Amy Sang. Complex role of matrix metalloproteinases in angiogenesis. Cell Research 1998;8:171-7.

[43] Tojo N, Asakura E, Koyama M, Tanabe T, Nakamura N. Effects of macrophage colony-stimulating factor (M-CSF) on protease production from monocyte, macrophage and foam cell in vitro: a possible mechanism for anti-atherosclerotic effect of M-CSF. Biochim Biophys Acta 1999;1452:275-84

[44] Gruber MF, Gerrard TL. Production of macrophage colony-stimulating factor (M-CSF) by human monocytes is differentially regulated by GM-CSF, TNF alpha, and IFN-gamma. Cell Immunol 1992;142:361-9.

[45] Fixe P, Praloran V. Macrophage colony-stimulating-factor (M-CSF or CSF-1) and its receptor: structure-function relationships. Eur Cytokine Netw 1997;8:125-36.

Figure legends

Fig. 1. *Summary of the results obtained in the proteomic characterization of hMSC-CM*

A. Venn diagram showing proteins detected in at least 3 out of 5 technical replicas in both patients only in stimulated hMSC-MC or unstimulated hMSC-CM or in both; B. t-test difference (difference of log(2) mean intensity of a protein in stimulated and unstimulated hMSC-CM replicas,[28]) observed in the two patients for the 57 proteins present in stimulated and unstimulated hMSC-MC

and significantly overrepresented in stimulated hMSC-MC according to t-test p-value (cut-off at 1% permutation-based False Discovery Rate). Pearson correlation coefficient R=0.73. Complete protein identities and detailed values are reported in Table 1.

Fig. 2. *Network interactions of overrepresented proteins in stimulated hMSC-CM involved in inflammation or in angiogenesis*. Overrepresented proteins in stimulated hMSC-CM involved in inflammation (A) or angiogenesis (B), respectively, according to targeted accurate literature mining as reported in Table 1, have been searched for possible interactions using String **[**34**]**. Active interactions: text mining, experiments, databases; edges thickness indicates "confidence". Red symbols: proteins present only in stimulated hMSC secretome or showing high t-test difference according to Fig. 1B. Yellow edges indicate proteins with proteases/protease inhibitors activity

Fig. 3. *Distribution into biological processes of the proteins overrepresented in stimulated hMSC-CM in human and mouse*. The proteins that were significantly up-regulated or present only in stimulated MSC-CM (Table 1 and [21]) were classified into different biological processes according to the Gene Ontology classification system (GOBP) using DAVID software [33]; confidence level: medium; only categories showing modified Fisher exact EASE score p value<0.05 and at least 5 counts in hMSC are represented. The bars represent the percentage of proteins involved in a category out of the total number of overrepresented proteins in human (96) or mouse (89) secretome. Asterisks indicate Fold Enrichment range for each category: * 1-5, ** 6-10, ***>10

Fig. 4: *Human and Mouse MSC conditioned media differentially stimulate monocytes differentiation.* A) Mouse bone marrow cells were cultured with murine M-CSF (as positive control), unstimulated or stimulated mouse MSC-CM for 5 days. Differentiation to macrophages was assessed by Flow Cytometry as percentage of F4/80+CD11b+ cells. Right panel: mouse M-CSF concentration in conditioned media was analysed by ELISA. Undetectable cytokine levels were reported for both preparations. B) Human PBMCs were cultured with human M-CSF (as positive control), unstimulated or stimulated human MSC-CM for 5 days. Macrophages were analysed by Flow Cytometry as CD14+ cells. Right panel: human M-CSF quantification by ELISA assay shows higher cytokine levels in st hMSC-CM than unst hMSC-CM. A and B, left panels: 3 independent experiments, data are expressed as mean ± SEM (*p<0.05, ****p<0.0001, One way Anova). A and B, right panels: 2 independent experiments, data are expressed as mean ± SEM (*p<0.05, parametric t-test).

Fig. 5. *Effect of Human or Mouse MSC conditioned medium on tube formation assay.* The effect of unstimulated or stimulated MSC media on endothelial cells was determined by a tube formation assay. Cells were seeded on the top of a matrigel phase in the presence of unstimulated or stimulated A) mouse, B) human MSC- CM. 6 hours later, images were acquired with a phase contrast inverted microscope at 4× objective magnification. Analysis was performed with ImageJ Angiogenesis Analyzer. A) SVEC4-10 network formation; quantification of the tube segment length (expressed in pixel number) and representative images at 4 hours. B) Huvec network formation; quantification of the tube segment length and representative images (expressed in pixel number) at 4 hours. 3 independent experiments, data are expressed as mean ± SEM (*$p<0.05$, **$p<0.01$, One way Anova).

Fig. 6***:*** *Timp-1 blocking reverts the anti-angiogenic effect of mouse and human MSC conditioned media.* In order to investigate the role of MSC-derived TIMP-1 on angiogenesis, the tube formation assay was performed in the presence of A) mouse or B) human TIMP-1 blocking antibody. Representative images of A) SVEC4-10 cell line or B) Huvec cells are taken with a phase contrast inverted microscope at 4× objective magnifications. Graphs show the quantification of the tube segment length measured with ImageJ Angiogenesis Analyzer. Data are expressed as mean ± SEM (*$p<0.05$, **$p<0.01$; One way Anova), 3 independent experiments.

Fig. 7. *Mouse and human MSC-derived TIMP-1 quantification*
MSC-derived TIMP-1 concentration in A) mouse and B) human unstimulated or stimulated MSC conditioned medium was measured with ELISA. Data are expressed as mean ± SEM (*$p<0.05$, parametric t-test), 2 independent experiments.

Table 1
Proteins overrepresented or present only in st hMSC-CM.

Gene names	Protein names	Protein ID	H30 -Log P *t*-test	H30 *t*-Test Diff[b]	H34 -Log P *t*-test	H34 *t*-Test Diff[b]	Angiogenesis[a]	Inflar
ABI3BP	Target of Nesh-SH3	D3YTG3	Only in stimulated					
AGRN	Agrin	O00468	5.339	2.799	3.970	1.066	x	x
ALCAM	CD166 antigen	Q13740	Only in stimulated				x	x
ARHGAP1	Rho GTPase-activating protein 1	Q07960	Only in stimulated					
BMP1	Bone morphogenetic protein 1	P13497	3.745	1.175	4.642	0.751	x	x
C1R	Complement C1r subcomponent	P00736	8.619	2.624	6.801	2.132		x
C1S	Complement C1s subcomponent	P09871	6.886	1.883	6.503	1.992		x
C3	Complement C3	P01024	10.267	7.920	5.001	4.683	x	x
CA12	Carbonic anhydrase 12	O43570	Only in stimulated				x	x
CCL2	C-C motif chemokine 2	P13500	9.381	6.120	10.273	9.600	x	x
CDC37	Hsp90 co-chaperone Cdc37	Q16543	Only in stimulated					x
CFB	Complement factor B	B4E1Z4	Only in stimulated				x	x
CFH	Complement factor H	P08603	5.941	2.293	6.526	2.405		x
CHI3L1	Chitinase-3-like protein 1	P36222	6.932	1.415	6.918	1.353	x	x
CLSTN1	Calsyntenin-1	O94985	4.674	0.615	3.190	0.932		
COL16A1	Collagen alpha-1(XVI) chain	A6NDR9	5.166	1.459	4.026	1.439		x
COL3A1	Collagen alpha-1(III) chain	P02461	7.283	0.588	10.347	1.865		x
COL5A2	Collagen alpha-2(V) chain	P05997	1.555	0.170	7.749	1.353		
COL7A1	Collagen alpha-1(VII) chain	Q02388	5.682	2.193	2.828	0.961		x
CSF1	Macrophage colony-stimulating factor 1	P09603	Only in stimulated				x	x
CTHRC1	Collagen triple helix repeat-cont prot 1	Q96CG8	5.339	1.314	4.189	1.134	x	
CTSB	Cathepsin B	P07858	3.149	0.636	5.472	1.500	x	x
CXCL1	Growth-regulated alpha protein	P09341	Only in stimulated				x	x
CXCL12	Stromal cell-derived factor 1	P48061	5.665	2.429	1.652	0.470	x	x
CXCL5	C-X-C motif chemokine 5	P42830	Only in stimulated				x	x
CXCL6	C-X-C motif chemokine 6	P80162	Only in stimulated				x	x
CYR61	Protein CYR61	O00622	Only in stimulated				x	x
DCN	Decorin	P07585	5.699	0.835	5.760	1.253	x	x
EFEMP2	EGF-cont fibulin-like extrac matrix prot 2	O95967	3.013	1.193	5.790	1.640		x
EIF6	Eukaryotic translation initiation factor 6	P56537	Only in stimulated				x	x
ELN	Elastin	F8WAH6	4.693	1.332	5.715	2.206	x	x
EXT1	Exostosin-1	Q16394	3.775	1.085	2.266	0.485		
EXT2	Exostosin-2	Q93063	Only in stimulated					
FBLN1	Fibulin-1	P23142	4.242	0.867	6.450	1.323	x	
FBN1	Fibrillin-1	P35555	6.035	0.969	6.557	1.909	x	x
FKBP1A	Peptidyl-prolyl cis trans isomerase	P62942	Only in stimulated					x
FN1	Fibronectin	P02751	5.787	0.793	5.421	0.358	x	x
FNDC1	Fibronectin type III domain-cont prot 1	Q4ZHG4	5.245	2.301	7.588	1.418	x	x
FSTL1	Follistatin-related protein 1	Q12841	3.823	0.817	7.039	1.968	x	x
GALNT2	Polypeptide *N*-acetylgalactosaminyltransferase 2	Q10471	2.914	0.542	2.860	0.895	x	
GBP1	Interferon-induced guanylate-binding prot 1	P32455	Only in stimulated				x	x
GC	Vitamin D-binding protein	P02774	Only in stimulated					x
HLA-A	HLA class I histocompatibility antigen, A-24 alpha chain	P05534	5.130	1.393	3.813	1.312		x
HLA-C	HLA class I histocompatibility antigen, Cw-7 alpha chain	A2AEA2	3.071	1.381	3.304	1.231		x
HSPG2	Base membr-spec hepar sulf proteoglycan core prot	P98160	8.735	1.796	9.468	2.141	x	x
HYOU1	Hypoxia up-regulated prot 1	Q9Y4L1	Only in stimulated				x	x
ICAM1	Intercellular adhesion molecule 1	P05362	Only in stimulated				x	x
IGFBP4	Insulin-like growth factor-binding prot 4	P22692	4.346	1.526	3.986	1.009	x	x
IGFBP6	Insulin-like growth factor-binding prot 6	P24592	Only in stimulated				x	x
IGFBP7	Insulin-like growth factor-binding prot 7	Q16270	2.725	0.397	4.650	0.947	x	x
IL6	Interleukin-6	P05231	Only in stimulated				x	x
IL8	Interleukin-8	P10145	Only in stimulated				x	x
INHBA	Inhibin beta A chain	P08476	7.879	3.140	5.875	1.448	x	
ITIH2	Inter-alpha-trypsin inhibitor heavy chain H2	P19823	3.742	1.104	1.276	0.382		x
ITM2B	Integral membrane protein 2B;BRI2	Q9Y287	3.573	1.994	5.351	1.035		
KRT6B	Keratin, type II cytoskeletal 6B	P04259	Only in stimulated					
LAMA4	Laminin subunit alpha-4	Q16363	2.027	0.234	1.925	0.173	x	
LAMB2	Laminin subunit beta-2	P55268	5.174	3.708	4.936	1.006		
LEPRE1	Prolyl 3-hydroxylase 1	Q32P28	Only in stimulated				x	x
LGALS3BP	Galectin-3-binding protein	Q08380	8.011	1.487	6.749	1.314	x	x
LOXL2	Lysyl oxidase homolog 2	Q9Y4K0	6.219	1.195	5.732	1.521	x	x
LYZ	Lysozyme C	P61626	3.547	0.507	1.328	0.607		x
MAN1A1	Mannosyl-oligosaccharide 1,2-alpha-mannosidase IA	P33908	Only in stimulated				x	x
MANBA	Beta-mannosidase	O00462	Only in stimulated					
MMP1	Interstitial collagenase	P03956	Only in stimulated				x	x
MMP10	Stromelysin-2	P09238	Only in stimulated				x	x
MMP13	Collagenase 3	G5E971	Only in stimulated				x	x
MMP2	72 kDa type IV collagenase	P08253	6.555	1.090	7.061	1.043	x	x
MMP3	Stromelysin-1	P08254	Only in stimulated				x	x
NID1	Nidogen-1	P14543	3.840	0.925	3.450	0.890	x	x
NID2	Nidogen-2	Q14112	4.384	1.133	3.823	0.855		
NUCB1	Nucleobindin-1	Q02818	5.878	0.985	3.867	0.703		
PLOD1	Procollagen-lysine,2-oxoglutarate 5-dioxygenase 1	B4DR87	3.944	0.876	2.180	0.264		
PLOD2	Procollagen-lysine,2-oxoglutarate 5-dioxygenase 2	O00469	5.967	2.636	5.402	2.331	x	

Table 1 (*continued*)

Gene names	Protein names	Protein ID	H30 -Log P *t*-test	H30 *t*-Test Diff[a]	H34 -Log P *t*-test	H34 *t*-Test Diff[a]	Angiogenesis[b]	Inflammation[b]
PSMA5	Proteasome subunit alpha type-5	P28066	Only in stimulated					
PSME2	Proteasome activator complex subunit 2	Q9UL46	Only in stimulated					
PTX3	Pentraxin-related protein PTX3	P26022	7.000	3.580	8.516	3.256	x	x
PXDN	Peroxidasin homolog	Q92626	6.359	1.401	5.119	1.122		
QPCT	Glutaminyl-peptide cyclotransferase	Q16769	3.070	1.972	4.593	2.140		x
QSOX1	Sulfhydryl oxidase 1	O00391	5.232	1.616	9.152	2.155	x	
RNASE4	Ribonuclease 4	P34096	Only in stimulated				x	x
SDC4	Syndecan-4	P31431	1.696	0.810	3.199	1.321	x	x
SDF4	45 kDa calcium-binding prot	Q9BRK5	2.014	0.353	3.547	0.862	x	
SERPINB2	Plasminogen activator inhibitor 2	P05120	Only in stimulated					x
SERPINE1	Plasminogen activator inhibitor 1	P05121	8.172	2.596	6.111	1.557	x	x
SLC39A14	Zinc transporter ZIP14	Q15043	Only in stimulated					
SLC3A2	4F2 cell-surface antigen heavy chain	P08195	Only in stimulated					
SOD2	Superoxide dismutase [Mn]	P04179	Only in stimulated				x	x
SRGN	Serglycin	P10124	5.249	1.412	3.353	1.084	x	
SRPX2	Sushi repeat-containing prot SRPX2	O60687	7.209	2.708	3.423	2.482	x	x
SSB	Lupus La protein	P05455	Only in stimulated					
STC2	Stanniocalcin-2	O76061	Only in stimulated				x	
TIMP1	Metalloproteinase inhibitor 1	P01033	2.940	1.254	5.763	1.081	x	x
TNC	Tenascin	P24821	6.040	1.645	7.257	1.329	x	x
TNFAIP6	Tumor necrosis factor-inducible gene 6 protein	P98066	Only in stimulated					x
VCAM1	Vascular cell adhesion protein 1	P19320	5.307	3.003	5.227	2.623	x	x

[a] *t*-Test diff: difference of log(2) mean intensity of a protein in technical replicas of st- versus unst hMSC-CM from *t*-test analysis using Perseus [28] as detailed in the text.
[b] Proteins related to angiogenesis or inflammation according to criteria detailed in "Materials and methods".

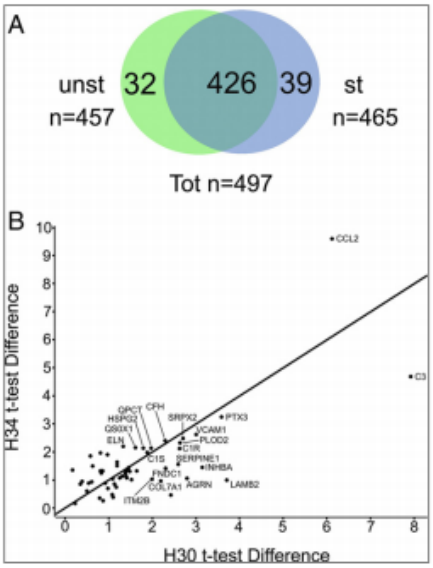

Fig. 1. Summary of the results obtained in the proteomic characterization of hMSC-CM. A. Venn diagram showing proteins detected in at least 3 out of 5 technical replicas in both patients only in stimulated hMSC-MC or unstimulated hMSC-CM or in both; B. t-test difference (difference of log(2) mean intensity of a protein in stimulated and unstimulated hMSC-CM replicas, [28]) observed in the two patients for the 57 proteins present in stimulated and unstimulated hMSC-MC and significantly overrepresented in stimulated hMSC-MC according to t-test p-value (cut-off at 1% permutation-based False Discovery Rate). Pearson correlation coefficient R = 0.73. Complete protein identities and detailed values are reported in Table 1.

Table 2
Proteins overrepresented or present only in st MSC-CM common to mouse and human.

Gene names	Protein names	Angiogenesis[a]	Infllammation[a]
AGRN	Agrin	x	x
C1R	Complement C1r subcomponent		x
C1S	Complement C1s subcomponent		x
C3	Complement C3	x	x
CSF1	Macrophage colony-stimulating factor 1	x	x
CTSB	Cathepsin B	x	x
CXCL1	Growth-regulated alpha protein	x	x
CXCL5	C-X-C motif chemokine 5	x	x
EXT1	Exostosin-1		
EXT2	Exostosin-2		
FSTL1	Follistatin-related protein 1	x	x
HSPG2	Basem membr-spec heparan sulfate proteoglycan core prot	x	x
IGFBP7	Insulin-like growth factor-binding protein 7	x	x
IL6	Interleukin-6	x	x
LAMB2	Laminin subunit beta-2		
LGALS3BP	Galectin-3-binding protein	x	x
MMP13	Collagenase 3	x	x
NID1	Nidogen-1	x	x
PLOD2	Procollagen-lysine,2-oxoglutarate 5-dioxygenase 2	x	
SERPINE1	Plasminogen activator inhibitor 1	x	x
TIMP1	Metalloproteinase inhibitor 1	x	x
TNC	Tenascin	x	x
VCAM1	Vascular cell adhesion protein 1	x	x

[a] Proteins involved in angiogenesis or inflammation in both organisms according to criteria detailed in "Materials and methods".

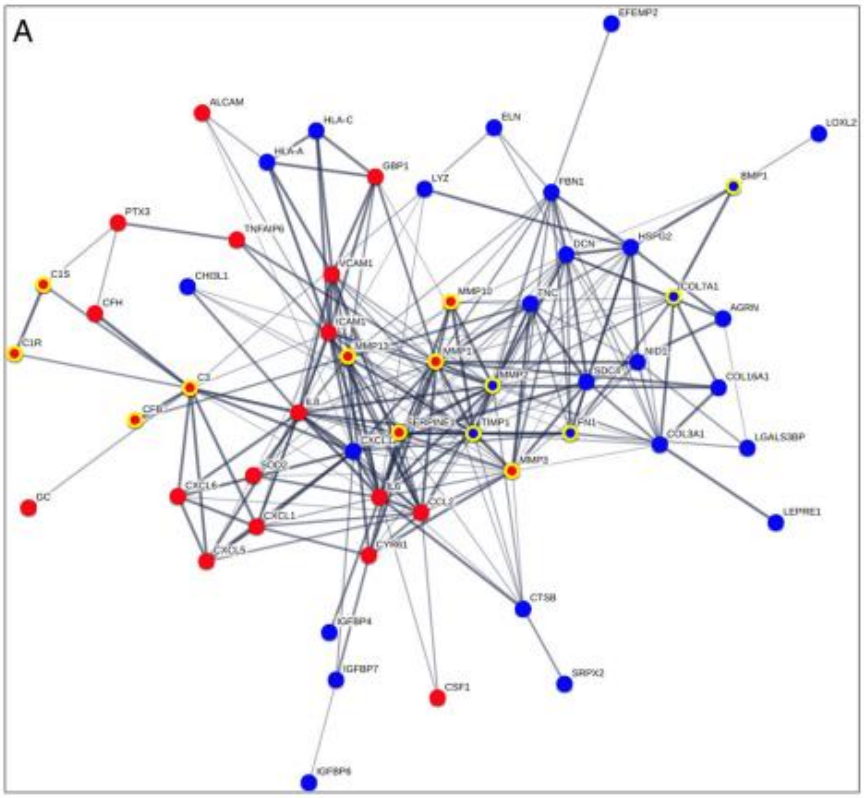
A
EFEMP2
ALCAM
HLA-C
ELN
LOXL2
HLA-A
GBP1
LYZ
FBN1
BMP1
PTX3
TNFAIP6
DCN
HSPG2
C1S
CHI3L1
VCAM1
MMP10
TNC
COL1A1
AGRN
CFH
ICAM1
C1R
MMP13
MMP1
NID2
C3
MMP7
SDC4
COL16A1
CFB
IL8
SERPINE1
TIMP1
PAI1
COL3A1
LGALS3BP
CXCL1
SOD2
MMP3
CXCL16
GC
IL6
CCL2
LEPRE1
CXCL1
CXCL5
CYR61
CTSB
IGFBP4
IGFBP7
CSF1
SRPX2
IGFBP6

680

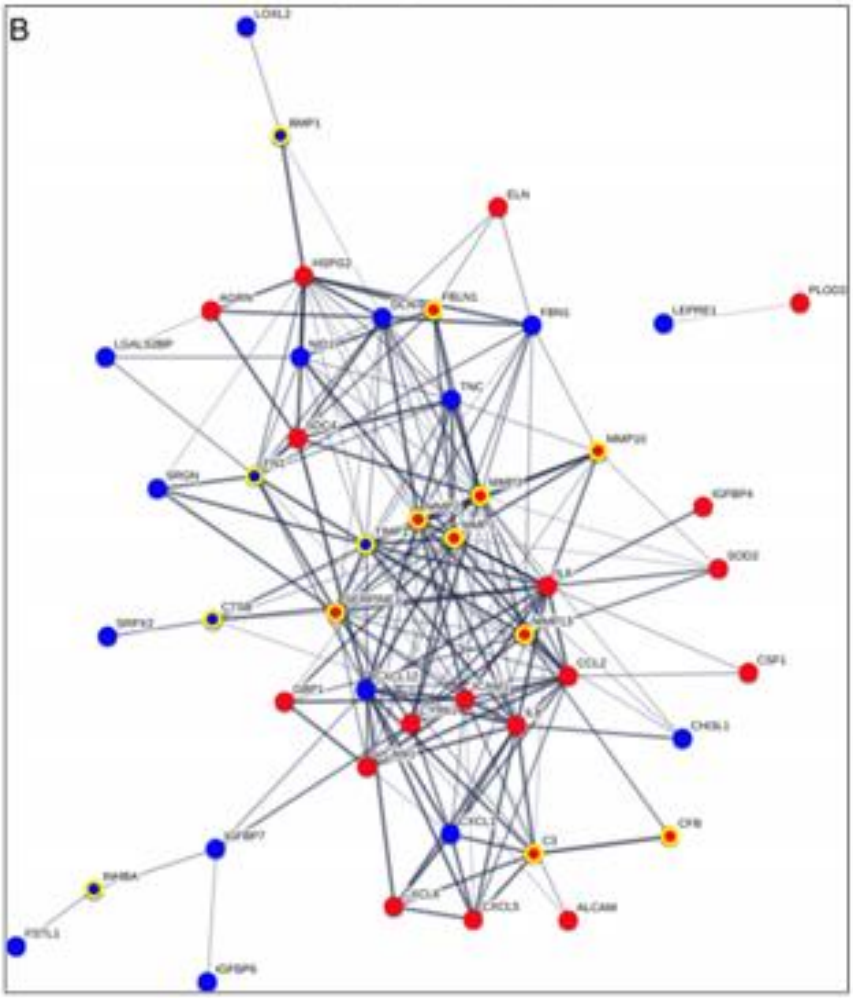
B
LOXL2
BMP1
ELN
HSPG2
AGRN
FBLN5
FBN1
LEPRE1
PLOD3
LGALS3BP
NID2
TNC
SDC4
MMP10
TN1
SPON
IGFBP4
SOD2
IL8
CTSB
SRPX2
CSF1
CCL2
GBP1
CHI3L1
CFB
IGFBP7
C3
RHBA
ALCAM
CXCL3
PSTL1
IGFBP6

681

Fig. 2. Network interactions of overrepresented proteins in stimulated hMSC-CM involved in inflammation or in angiogenesis. Overrepresented proteins in stimulated hMSC-CM involved in inflammation (A) or angiogenesis (B), respectively, according to targeted accurate literature mining as reported in Table 1, have been searched for possible interactions using String [34]. Active interactions: text mining, experiments, databases; edges thickness indicates “confidence”. Red symbols: proteins present only in stimulated hMSC secretome or showing high t-test difference according to Fig. 1B. Yellow edges indicate proteins with proteases/protease inhibitors activity.

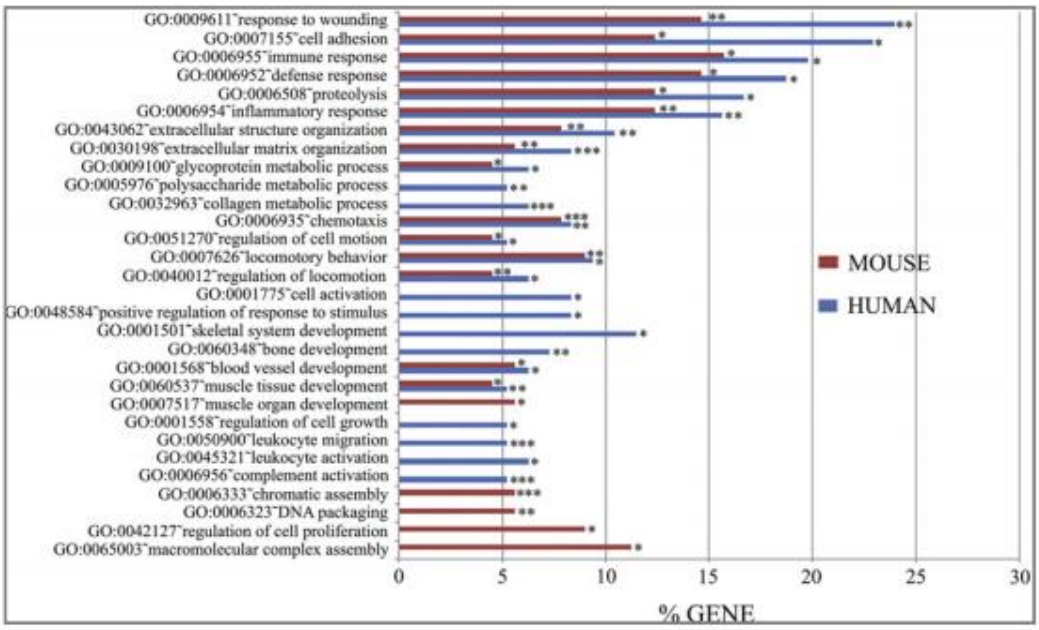

Fig. 3. Distribution into biological processes of the proteins overrepresented in stimulated hMSC-CM in human and mouse. The proteins that were significantly up-regulated or present only in stimulated MSC-CM (Table 1 and [21]) were classified into different biological processes according to the Gene Ontology classification system (GOBP) using DAVID software [33];confidence level: medium; only categories showing modified Fisher exact EASE score p value b 0.05 and at least 5 counts in hMSC are represented. The bars represent the percentage of proteins involved in a category out of the total number of overrepresented proteins in human (96) or mouse (89) secretome. Asterisks indicate fold enrichment range for each category: * 1–5, ** 6–10, *** N 10.

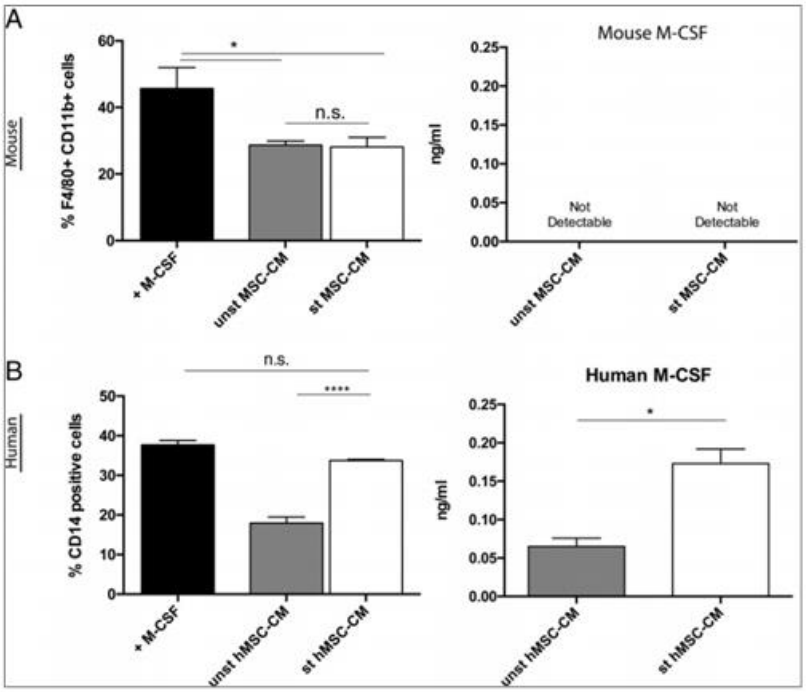

Fig. 4. Human and mouse MSC conditioned media differentially stimulate monocytes differentiation. A) Mouse bone marrow cells were cultured with murine M-CSF (as positive control), unstimulated or stimulated mouse MSC-CM for 5 days. Differentiation to macrophages was assessed by Flow Cytometry as percentage of F4/80 + CD11b + cells. Right panel: mouse M-CSF concentration in conditioned media was analysed by ELISA. Undetectable cytokine levels were reported for both preparations. B) Human PBMCs were cultured with human M-CSF (as positive control), unstimulated or stimulated human MSC-CM for 5 days. Macrophages were analysed by Flow Cytometry as CD14 + cells. Right panel: humanM-CSFquantification by ELISA assay shows higher cytokine levels in st hMSC-CM than unst hMSC-CM. A and B, left panels: 3 independent experiments, data are expressed as mean ± SEM (*p b 0.05, ****p b 0.0001, One way ANOVA). A and B, right panels: 2 independent experiments, data are expressed as mean ± SEM (*p b 0.05, parametric t-test).

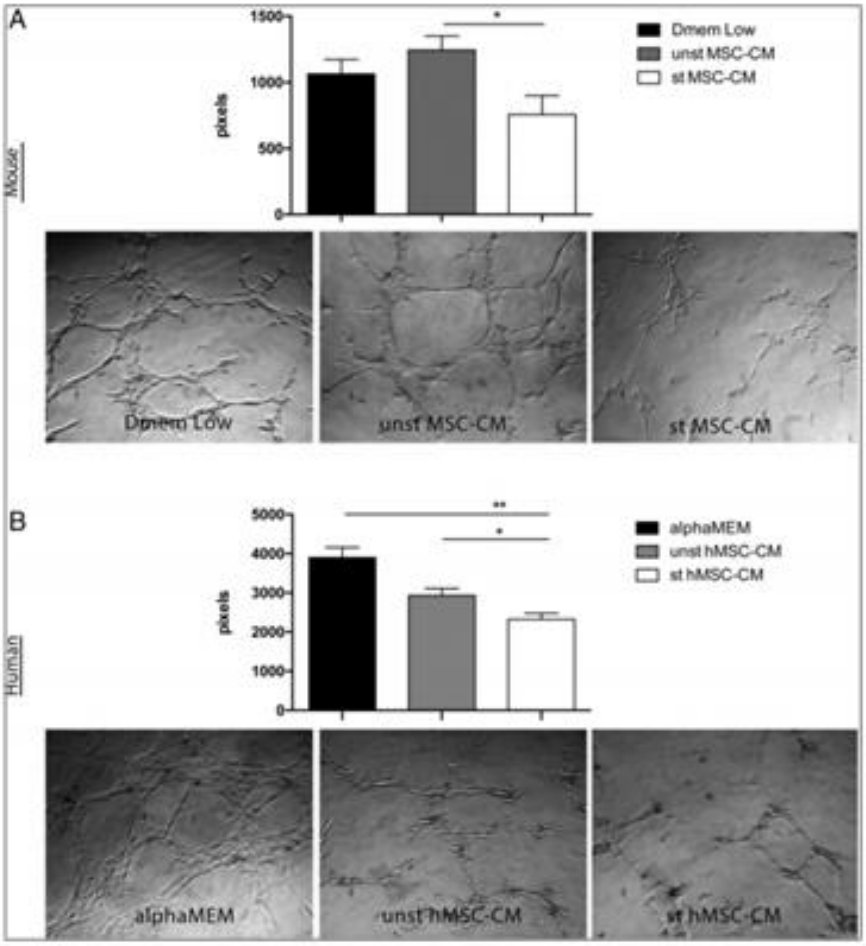

Fig. 5. Effect of human or mouse MSC conditioned medium on tube formation assay. The effect of unstimulated or stimulated MSC media on endothelial cells was determined by a tube formation assay. Cells were seeded on the top of a matrigel phase in the presence of unstimulated or stimulated A) mouse, B) human MSC-CM. 6 h later, images were acquired with a phase contrast inverted microscope at 4 × objective magnification. Analysis was performed with ImageJ Angiogenesis Analyzer. A) SVEC4-10 network formation; quantification of the tube segment length (expressed in pixel number) and representative images at 4 h. B) Huvec network formation; quantification of the tube segment length and representative images (expressed in pixel number) at 4 h. 3 independent experiments, data are expressed as mean ± SEM (*p b 0.05, **p b 0.01, One way ANOVA).

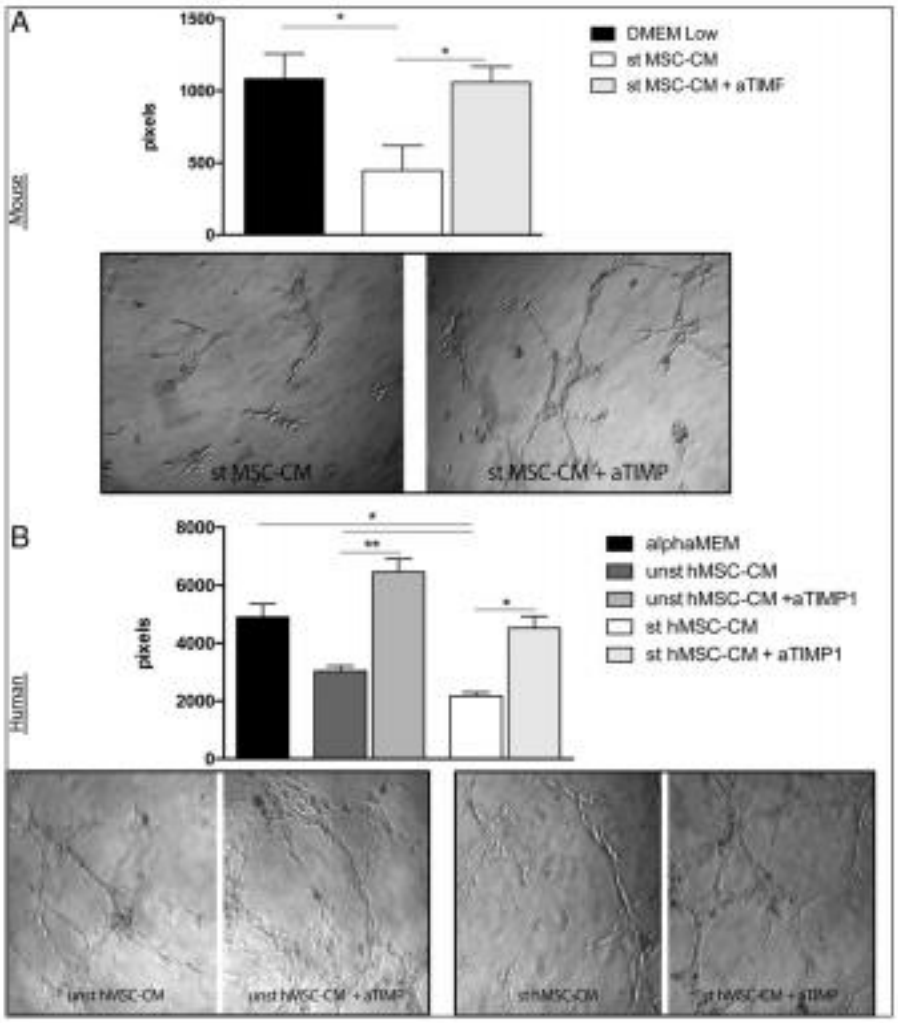

Fig. 6. Timp-1 blocking reverts the anti-angiogenic effect of mouse and human MSC conditioned media. In order to investigate the role of MSC-derived TIMP-1 on angiogenesis, the tube formation assay was performed in the presence of A) mouse or B) human TIMP-1 blocking antibody. Representative images of A) SVEC4-10 cell line or B) Huvec cells are taken with a phase contrast inverted microscope at 4 × objective magnifications. Graphs show the quantification of the tube segment length measured with ImageJ Angiogenesis Analyzer. Data are expressed as mean ± SEM (*p b 0.05, **p b 0.01; One way ANOVA), 3 independent experiments.

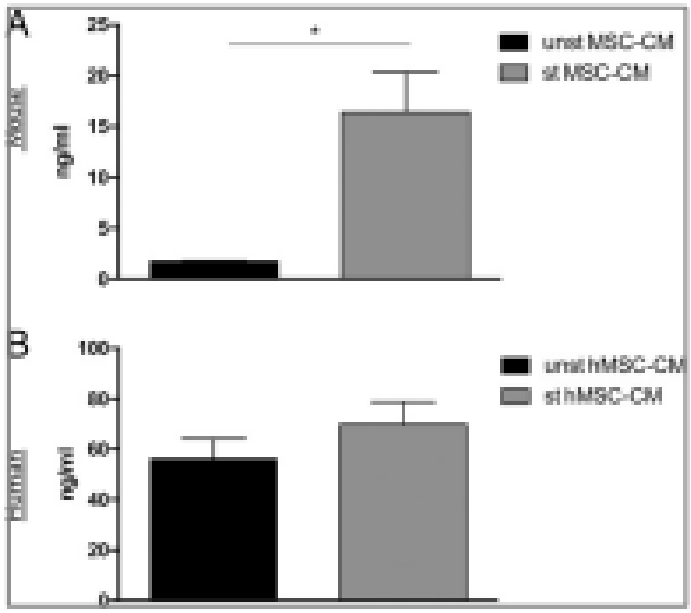

Fig. 7. Mouse and human MSC-derived TIMP-1 quantification. MSC-derived TIMP-1 concentration in A) mouse and B) human unstimulated or stimulated MSC conditioned medium was measured with ELISA. Data are expressed as mean ± SEM (*p b 0.05, parametric t-test), 2 independent experiments.